PCCP

PAPER

Cite this: *Phys. Chem. Chem. Phys.*, 2014, **16**, 5536

Adsorption of PNIPAm$_x$-PEO$_{20}$-PPO$_{70}$-PEO$_{20}$-PNIPAm$_x$ pentablock terpolymer on gold surfaces: effects of concentration, temperature, block length, and surface properties

Tongquan Chen, Yanping Lu, Tianyou Chen, Xinghong Zhang and Binyang Du*

The effects of concentration, relative block length and environmental temperature as well as the surface chemical and wetting properties of solid substrates on the adsorption behaviors and mechanisms of a series of pentablock terpolymer poly(*N*-isopropylacrylamide)$_x$-poly(ethylene oxide)$_{20}$-poly(propylene oxide)$_{70}$-poly(ethylene oxide)$_{20}$-poly(*N*-isopropylacrylamide)$_x$ (PNIPAm$_x$-PEO$_{20}$-PPO$_{70}$-PEO$_{20}$-PNIPAm$_x$ or PNIPAm$_x$-P123-PNIPAm$_x$) with x of 10, 63 and 97 on gold were studied by using a quartz crystal microbalance (QCM) technique. It was found that increasing the solution concentration did not alter the adsorption mechanism of thickness growth mode but increase the adsorption amount of PNIPAm$_{97}$-P123-PNIPAm$_{97}$ on a bare gold substrate at 20 °C. Increasing the length x of PNIPAm block decreased the adsorption rate constant and shifted the adsorption mechanism from the densification adsorption process for PNIPAm$_{10}$-P123-PNIPAm$_{10}$ to the thickness growth mode for PNIPAm$_{63}$-P123-PNIPAm$_{63}$ and PNIPAm$_{97}$-P123-PNIPAm$_{97}$ on bare (unmodified) gold substrate at 20 °C. The adsorption mechanisms of PNIPAm$_{97}$-P123-PNIPAm$_{97}$ at 20 °C on the hydrophobic and hydrophilic gold surfaces were the thickness growth mode and densification adsorption process, respectively. A complex adsorption behavior with large adsorption amounts was observed at the lower critical solution temperature (LCST) of PNIPAm block, *i.e.* 34.7 °C, for the adsorption of PNIPAm$_{97}$-P123-PNIPAm$_{97}$ not only on hydrophobic gold substrates but also on hydrophilic gold substrates. The adsorption mechanism of PNIPAm$_{97}$-P123-PNIPAm$_{97}$ micelles at 45 °C was the densification adsorption process regardless of the surface wetting and chemical properties of gold substrate. Overall, the adsorption behavior and mechanism of PNIPAm$_x$-P123-PNIPAm$_x$ pentablock terpolymers were mainly determined by the interactions of the pentablock terpolymers with different chain conformations in dilute aqueous solutions at various temperatures and the gold substrates with surface wetting and chemical properties.

Received 27th October 2013,
Accepted 20th December 2013

DOI: 10.1039/c3cp54535k

www.rsc.org/pccp

Introduction

The adsorption behavior of polymers at solid–liquid interfaces is a long-standing research hot-topic because it is relevant to many technological applications and biological processes.[1–20] In the past decades, the adsorption behavior of homo-polymers, diblock and triblock copolymers has been investigated in depth because of their relatively simple chain structures.[1–20] More recently, attention has also been paid to the adsorption behavior of multiblock copolymers at solid–liquid interfaces.[21–27] The multiblock copolymers possess many blocks, of which the chemical structure and physical properties could be independently controlled. The multiblock copolymers could have multiple block-functionalities and chain conformations. The investigations of chain conformations and adsorption behaviors of multiblock copolymers are thought to be helpful for understanding of the structure–property relationship of biomacromolecules, such as DNA and protein, which consist of multiple building blocks like base pairs and amino acids.

Theoretical studies and computer simulations have been carried out to study the adsorption behavior of multiblock copolymers at solid–liquid interfaces. Bhattacharya *et al.*[21] studied the adsorption of a single multiblock AB copolymer on a solid planar substrate by means of computer simulations and scaling analysis and found that the critical adsorption energy and the fraction of adsorbed monomers were related to the block length of sticking monomers and the total length of the multiblock copolymer chains. Sumithra *et al.*[27] used Monte Carlo simulations to study the adsorption of a system of multiblock copolymers having two different types of monomer

MOE Key Laboratory of Macromolecular Synthesis and Functionalization, Department of Polymer Science & Engineering, Zhejiang University, Hangzhou 310027, China. E-mail: duby@zju.edu.cn

units and various block lengths on a series of checker board surface configurations with various chess board square dimensions. They observed an intermediate size of the square on the board where the recognition and pinning are most favored and for a smaller and larger size of the board and block length, adsorption proceeds like in homopolymer on homogeneous surfaces. They also found that the conformational properties of the multiblock copolymer near the checkered surface show interesting effects with the perpendicular component, showing strong deviations from the standard behavior. Kriksin *et al.*[26] proposed a statistical mechanical model to investigate the adsorption of periodic multiblock copolymers $(A_lB_l)_x$ on chemically heterogeneous surfaces with regularly distributed stripes of two types (A and B). It is assumed that A(B)-type segments selectively adsorb onto A(B)-type stripes. They found that adsorption strongly depends on the copolymer sequence distribution and the arrangement of selectively adsorbing regions on the surface and the polymer-surface binding proceeds as a two-step process. The adsorption behavior of hydrophobic-polar regular multiblock copolymers at a selective solvent–solvent interface with emphasis on the impact of block length M on the copolymer adsorption behavior was also investigated by theoretical and simulation methods.[25,28]

However, experimental studies of the adsorption behavior of multiblock copolymers at the solid–liquid interfaces are still rare.[23,24] Liu *et al.*[23] studied the adsorption behavior of a pentablock terpolymer, poly(2-dimethylaminoethyl methacrylate)-poly(ethylene oxide)-poly(propylene oxide)-poly(ethylene oxide)-poly(2-dimethylaminoethyl methacrylate) ($PDMAEMA_{24}$-PEO_{132}-PPO_{50}-PEO_{132}-$PDMAEMA_{24}$) on various solid substrates with different surface charges and wetting properties (polypropylene, cellulose, and silica) using quartz crystal microbalance (QCM) and surface plasmon resonance (SPR). The authors correlated the observed adsorption behavior on various solid substrates with the effects of electrostatic screening, polymer hydrodynamic size, and solvency. More experimental, theoretical and simulation studies are strongly needed for further understanding and illustrating the adsorption behavior and mechanism of multiblock copolymers at solid–liquid interfaces. In the present work, the adsorption behavior of a series of thermally sensitive $PNIPAm_x$-PEO_{20}-PPO_{70}-PEO_{20}-$PNIPAm_x$ ($PNIPAm_x$-P123-$PNIPAm_x$) pentablock terpolymers with various lengths x of the PNIPAm block on the gold substrates were experimentally investigated using a quartz crystal microbalance (QCM) technique. The effects of concentration, relative block length and environmental temperatures as well as the surface chemical and wetting properties of the gold substrates on their adsorption behavior and mechanism were discussed.

Experimental

Chemical and materials

Three pentablock terpolymers, $PNIPAm_x$-P123-$PNIPAm_x$ with various PNIPAm block length x, were studied in the present work, which were previously synthesized by ATRP with NIPAm as the monomer and modified P123 as the macroinitiator (Table 1).[29,30]

Table 1 Number-averaged molecular weight M_n and molecular weight distribution M_w/M_n of the three $PNIPAm_x$-P123-$PNIPAm_x$ pentablock terpolymers[30]

Pentablock terpolymers	M_n [a] ($\times 10^3$ g mol^{-1})	M_n [b] ($\times 10^3$ g mol^{-1})	M_w/M_n [b]
$PNIPAm_{10}$-P123-$PNIPAm_{10}$	8.3	11.4	1.34
$PNIPAm_{63}$-P123-$PNIPAm_{63}$	20.2	21.7	1.65
$PNIPAm_{97}$-P123-$PNIPAm_{97}$	28.0	29.3	1.69

[a] Determined from ^{1}H-NMR. [b] Determined from GPC with DMF and 0.05 M LiBr as eluent and monodisperse poly(methyl methacrylate) as the calibration standard.

The pentablock terpolymers, $PNIPAm_x$-P123-$PNIPAm_x$, were dissolved in de-ionized water to give a concentration of 0.5 mg ml^{-1} for the adsorption measurements, respectively. For $PNIPAm_{97}$-P123-$PNIPAm_{97}$, aqueous solutions with concentrations of 0.1 and 0.3 mg ml^{-1} were also prepared.

Modification of gold-electrodes of quartz crystals

The surface properties of the gold electrode of the quartz crystal could be modified by self-assembling a monolayer of thiols. 1-Dodecanethiol ($HS(CH_2)_{11}CH_3$) and 11-mercaptoundecanol ($HS(CH_2)_{11}OH$) were used in the present work in order to obtain well-defined hydrophobic and hydrophilic gold surfaces, respectively.[15] The new gold-coated quartz crystals were unpacked and immersed into piranha solution (3 : 7 mixture of 30% H_2O_2 and concentrated H_2SO_4) for 10 min, followed by rinsing with copious de-ionized water three times and drying with nitrogen. (**Caution!** Piranha solution is a very strong oxidizing agent and reacts violently with organic compounds. It should be handled with extreme care.) The quartz crystals were then immersed in ethanol solution (1 mM) of 1-dodecanethiol ($HS(CH_2)_{11}CH_3$) or 11-mercaptoundecanol ($HS(CH_2)_{11}OH$) for 18 h. Afterwards, the treated quartz crystals were taken out of the thiol solution, followed by rinsing with copious ethanol three times and drying with nitrogen. The static water contact angles of the 1-dodecanethiol and 11-mercaptoundecanol modified gold surfaces were *ca.* $108 \pm 1^\circ$ and $25 \pm 2^\circ$, respectively, which were consistent with the reported values.[15] Hence, the 1-dodecanethiol modified gold surface was hydrophobic, whereas the 11-mercaptoundecanol modified gold surface was hydrophilic. The thiol-modified quartz crystals were then stored in ethanol before use.

Contact angle measurements

The static contact angles of the newly-unpacked and modified gold surfaces were measured for the unmodified and modified quartz crystals using a contact angle meter OCA20 (Dataphysics Inc., Germany). 1 μL sessile droplets were placed on the surface of a gold electrode and the shape of the droplet was recorded for calculating the static contact angle. Three measurements on different spots of the given quartz crystal were carried out to obtain the average contact angle of the gold electrode.

QCM adsorption measurements of $PNIPAm_x$-P123-$PNIPAm_x$

The effects of solution concentration, temperature, PNIPAm block length x and the surface wetting properties of gold electrode on

the adsorption behaviors of the pentablock terpolymer PNIPAm$_x$-P123-PNIPAm$_x$ were investigated using a quartz crystal microbalance (QCM, Resonant Probes GmbH, Goslar, Germany). AT-cut quartz crystals with a fundamental resonant frequency f_0 of 5 MHz and gold electrodes were used (Hangzhou Dongwei Inc., Hangzhou, China). Note that the static water contact angle of the gold surface of the newly-unpacked quartz crystal was *ca.* 101 ± 3°, indicating that the bare (unmodified) gold surface was hydrophobic.[24] Typically, the quartz crystal was installed in the QCM's liquid cell with temperature control and a stable baseline was established in the flow of de-ionized water with a flow rate of 50 μl min^{-1}. The de-ionized water was then replaced with the aqueous solution of the pentablock terpolymer PNIPAm$_x$-P123-PNIPAm$_x$. The frequency and half-band-half shifts of quartz crystal at the 3rd overtone were recorded *vs.* time until equilibrium in adsorption was clearly observed unless otherwise stated. The quartz crystal was then rinsed with de-ionized water by replacing the terpolymer solution with de-ionized water. After rinsing, the quartz crystal with adsorbed pentablock terpolymer layer was taken out and dried with nitrogen. Note that the 3rd overtone was chosen for the QCM measurements because of the sufficient energy trapping at 3rd overtone of the quartz crystal operating in liquid.[31]

Results and discussion

Effect of solution concentration

Fig. 1A shows the frequency ($\Delta f_3/3$) and half-band-half width ($\Delta\Gamma_3/3$) shifts of the quartz crystals during the adsorption of PNIPAm$_{97}$-P123-PNIPAm$_{97}$ onto the bare hydrophobic gold surface at 20 °C with various terpolymer concentrations of 0.1, 0.3 and 0.5 mg mL^{-1}. Note that the bare gold surface of the quartz crystal was hydrophobic with a contact angle of 101 ± 3°. It can be seen that increasing the solution concentration led to increase of the adsorption amount of PNIPAm$_{97}$-P123-PNIPAm$_{97}$ at equilibrium and after rinsing. Furthermore, the buildup process of PNIPAm$_{97}$-P123-PNIPAm$_{97}$ adsorbed layers was independent of the solution concentrations studied here, as shown in Fig. 1B. It could be seen from Fig. 1B that the evolution of $\Delta\Gamma_3/3$ as a function of $-\Delta f_3/3$ was overlapped for the adsorption processes of PNIPAm$_{97}$-P123-PNIPAm$_{97}$ with various concentrations onto the bare (unmodified) hydrophobic gold surfaces at 20 °C. A linear relation of $\Delta\Gamma_3/3$ and $-\Delta f_3/3$ was also clearly observed for the adsorption processes of PNIPAm$_{97}$-P123-PNIPAm$_{97}$. Such linear relation of $\Delta\Gamma$ to $-\Delta f$ indicated that the viscoelastic properties of the adsorbed PNIPAm$_{97}$-P123-PNIPAm$_{97}$ thin film remained unchanged during the film growth and the growth of the adsorbed PNIPAm$_{97}$-P123-PNIPAm$_{97}$ thin film occurred *via* a thickness growth mode.[8,9,14] Since the bare gold surface is hydrophobic and both the gold surface and the pentablock terpolymer are not charged, the driving force for the adsorption of PNIPAm$_x$-P123-PNIPAm$_x$ on bare gold surface was complex and might include van der Waals' interaction and hydrophobic interaction. The inset of Fig. 1B shows that the negative frequency shift ($-\Delta f_3/3$) after rinsing was linear with the concentrations of PNIPAm$_{97}$-P123-PNIPAm$_{97}$ aqueous solutions studied here, which further supported the thickness growth mode. Therefore, a concentration of 0.5 mg mL^{-1} was chosen for the following experiments in order to correlate the adsorption behavior of the pentablock terpolymers with their chain conformations in aqueous solutions with the same concentration, as revealed by dynamic light scattering (DLS).[30]

Effect of adsorption temperature

Previous studies showed that the chain conformations of PNIPAm$_x$-P123-PNIPAm$_x$ and PNIPAm$_{110}$-F127-PNIPAm$_{110}$ pentablock terpolymers in dilute aqueous solutions were strongly dependent on the solution temperatures.[29,30] Two LCSTs were observed for these PNIPAm-PEO-PPO-PEO-PNIPAm pentablock terpolymers in dilute aqueous solutions, which were corresponding to the LCSTs of PPO and PNIPAm blocks, respectively. At temperatures below the LCST of PPO block (like 20 °C), such pentablock terpolymers formed "associate" structures, whereas micelles with hydrophobic PNIPAm and PPO blocks as cores and soluble PEO blocks as coronas were formed at temperatures above the LCST of PNIPAm block (like 45 °C). The chain conformation of polymers will strongly affect their adsorption

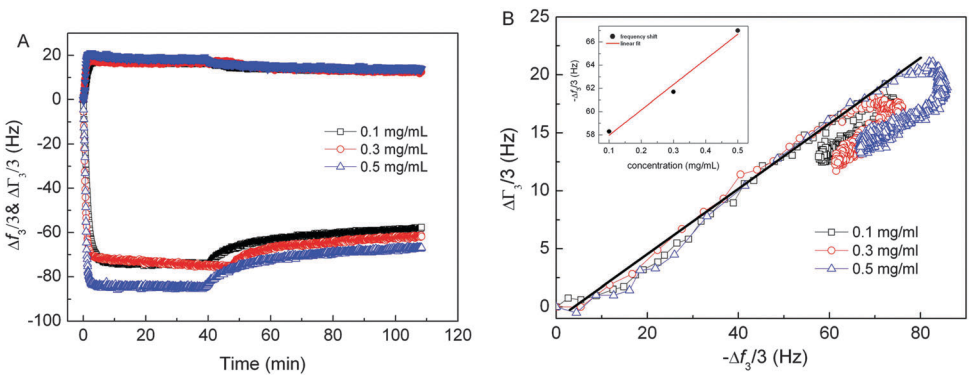

Fig. 1 (A) Frequency shift ($\Delta f_3/3$, open symbols) and half-band half-width shift ($\Delta\Gamma_3/3$, solid symbols) of the quartz crystals during the adsorption of PNIPAm$_{97}$-P123-PNIPAm$_{97}$ onto the bare hydrophobic gold surface at 20 °C with various concentrations. (B) The corresponding plots of half-band-half width shift $\Delta\Gamma_3/3$ *versus* negative frequency shift $-\Delta f_3/3$. The solid line was the guide to the eyes. The inset of (B) shows the frequency shifts after rinsing as a function of concentration of PNIPAm$_{97}$-P123-PNIPAm$_{97}$ aqueous solution.

behavior onto the solid substrates. The adsorption behavior of $PNIPAm_{110}$-F127-$PNIPAm_{110}$ onto a bare hydrophobic gold surface was previously confirmed to be strongly dependent on the solution temperatures, *i.e.* the chain conformation in aqueous solution.[24] In the present work, the effects of solution temperatures on the adsorption of $PNIPAm_{97}$-P123-$PNIPAm_{97}$ were further investigated in details.

Fig. 2 and 3 show the frequency ($\Delta f_3/3$) shifts of the quartz crystals and the corresponding plots of $\Delta\Gamma_3/3$ *versus* $-\Delta f_3/3$ during the adsorption of $PNIPAm_{97}$-P123-$PNIPAm_{97}$ onto the bare hydrophobic gold surface at various temperatures. Note that the LCSTs of PPO and PNIPAm blocks were *ca.* 29 °C and 34.7 °C, respectively, for $PNIPAm_{97}$-P123-$PNIPAm_{97}$ pentablock terpolymer in dilute aqueous solution.[30] The LCST of PPO block of $PNIPAm_x$-P123-$PNIPAm_x$ pentablock terpolymers was also dependent on the length of the PNIPAm block. The LCST of PPO block shifted from 24.4 to 29 °C when the length x of PNIPAm block increased from 10 to 97.[30] The adsorption amount, which could be qualitatively referred by $\Delta f_3/3$ after rinsing, increased with increasing the solution temperature, reached the maximum at the LCST of PNIPAm block, *i.e.* 34.7 °C, and then decreased with further increasing temperature, as shown in the inset of Fig. 2A. Two evolution regimes of adsorption behavior could be then identified for the temperature range of 20 to 45 °C. The first regime was from 20 to 34.7 °C. It can be clearly observed that the adsorption behavior of $PNIPAm_{97}$-P123-$PNIPAm_{97}$ deviated from the thickness growth mode with increasing the solution temperature from 20 to 29 °C. At higher temperature of 32 °C, the deviation was more manifest. More times were required to reach adsorption equilibrium at higher temperatures. The slopes of $\Delta\Gamma_3/3$ to $-\Delta f_3/3$ plots bended to lower value when increasing the solution temperature from 20 to 32 °C, indicating that the adsorbed pentablock terpolymer layers obtained at higher temperature were soften (Fig. 3A). Continuous adsorption of $PNIPAm_{97}$-P123-$PNIPAm_{97}$ was observed in the experimental time scale of *ca.* 120 min at 34.7 °C. The plot of $\Delta\Gamma_3/3$ *versus* $-\Delta f_3/3$ showed irregular behavior as shown in Fig. 3B. Negative value of $\Delta\Gamma_3$ was even observed at the long adsorption time. Similar complex adsorption behavior was previously observed for $PNIPAm_{110}$-F127-$PNIPAm_{110}$ at the corresponding LCST of PNIPAm block, *i.e.* 34 °C.[24] Liu *et al.*[23] also observed a maximum in adsorption of $PDMAEMA_{24}$-PEO_{132}-PPO_{50}-PEO_{132}-$PDMAEMA_{24}$ pentablock terpolymer onto the hydrophobic polypropylene (PP) surface around the critical micelle concentration (cmc). Note that PDMAEMA presented poly(2-dimethylaminoethyl methacrylate). Malmsten *et al.*[17] found that the adsorbed amount of PEO-PPO-PEO (Pluronic) block copolymers at untreated silica surfaces increased dramatically just prior to the critical micellization temperature (cmt) where it leveled off.

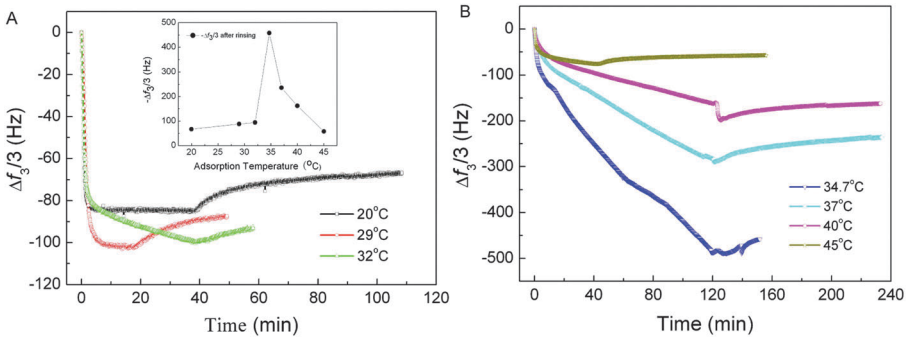

Fig. 2 Frequency shifts ($\Delta f_3/3$) of the quartz crystals during the adsorption of $PNIPAm_{97}$-P123-$PNIPAm_{97}$ onto the bare hydrophobic gold surface at various temperatures. (A) 20, 29 and 32 °C; (B) 34.7, 37, 40 and 45 °C. The inset of (A) showed the $\Delta f_3/3$ after rinsing as a function of adsorption temperature. The concentration of $PNIPAm_{97}$-P123-$PNIPAm_{97}$ aqueous solution was 0.5 mg mL^{-1}.

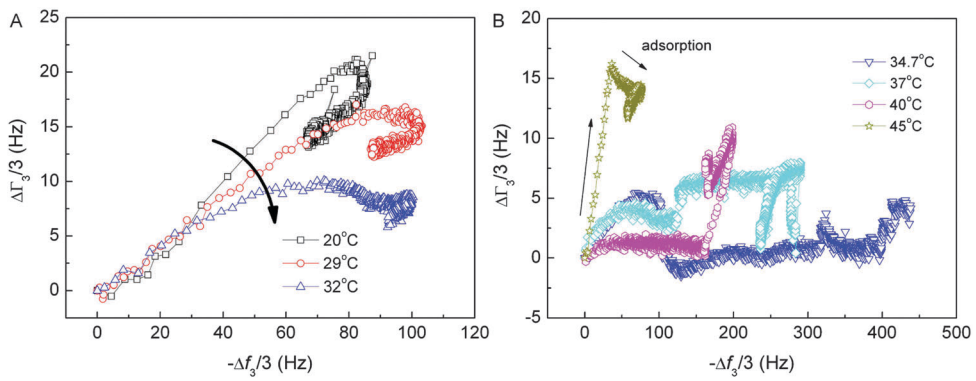

Fig. 3 The corresponding plots of $\Delta\Gamma_3/3$ *versus* $-\Delta f_3/3$ for the adsorption of $PNIPAm_{97}$-P123-$PNIPAm_{97}$ onto the bare hydrophobic gold surface at various temperatures. (A) 20, 29 and 32 °C; (B) 34.7, 37, 40 and 45 °C.

The PNIPAm-PEO-PPO-PEO-PNIPAm pentablock terpolymers started to form micelles with collapsed PPO and PNIPAm cores and swollen PEO shells at the LCST of PNIPAm block, which was similar to the cases of PDMAEMA-PEO-PPO-PEO-PDMAEMA at cmc and PEO-PPO-PEO at cmt. The premicellar associative adsorption could be used to account for the large adsorption observed at cmc for the case of PDMAEMA-PEO-PPO-PEO-PDMAEMA or at the LCST of PNIPAm block for the cases of $PNIPAm_{110}$-F127-$PNIPAm_{110}$ (*i.e.* 34 °C) and $PNIPAm_{97}$-P123-$PNIPAm_{97}$ (*i.e.* 34.7 °C), where the terpolymer micelles started to be formed. The surface association might take place just prior to solution micellization, giving rise to the strong increase of the adsorbed amount.[17,18,24,32,33]

The second evolution regime of adsorption behavior of $PNIPAm_{97}$-P123-$PNIPAm_{97}$ on bare hydrophobic gold surface was from 34.7 to 45 °C. Further increasing the solution temperature from 34.7 to 45 °C, the adsorption behavior was slowly changed from the complex process at 34.7 °C to a clear densification adsorption process at 45 °C (Fig. 3B). For the densification adsorption behavior, the $\Delta\Gamma_3/3$ first increased with $-\Delta f_3/3$ and then decreased during adsorption process as shown in Fig. 3B, indicating that the rigidity of adsorbed terpolymer layer increased with further adsorption.[13] However, continuous adsorption processes in 120 min were still observed at 37 and 40 °C. Interestingly, the extent and adsorption amounts were much less than that observed at 34.7 °C. A densification adsorption process was observed at 45 °C for the adsorption of $PNIPAm_{97}$-P123-$PNIPAm_{97}$ (Fig. 3B). Previously, a densification adsorption behavior was already observed at a lower temperature of 40 °C for the adsorption of $PNIPAm_{110}$-F127-$PNIPAm_{110}$ onto a bare hydrophobic gold surface.[24] These phenomena might be explained by the relative block lengths of $PNIPAm_{110}$-F127-$PNIPAm_{110}$ and $PNIPAm_{97}$-P123-$PNIPAm_{97}$. The lengths of PPO and PNIPAm blocks were similar for both of $PNIPAm_{110}$-F127-$PNIPAm_{110}$ and $PNIPAm_{97}$-P123-$PNIPAm_{97}$. However, the length of hydrophilic PEO block was only 20 for $PNIPAm_{97}$-P123-$PNIPAm_{97}$, which was much shorter than that of 100 for $PNIPAm_{110}$-F127-$PNIPAm_{110}$. The shorter hydrophilic PEO block had higher energy penalty and difficulty of bending in the formation of hydrophilic loops so that the higher temperature might be required to form the stable core–shell micelles for $PNIPAm_{97}$-P123-$PNIPAm_{97}$. Micellar associations might still occur during the adsorption process at temperatures of 37 and 40 °C, accounting for the continuous adsorption processes observed at 37 and 40 °C (Fig. 2B). At temperature where stable core–shell micelles were formed, the adsorption of stable $PNIPAm_{110}$-F127-$PNIPAm_{110}$ or $PNIPAm_{97}$-P123-$PNIPAm_{97}$ core–shell micelles onto bare hydrophobic gold surface exhibited a densification adsorption process.[24]

Effect of length *x* of PNIPAm block

Fig. 4 shows the adsorption behavior of $PNIPAm_x$-P123-$PNIPAm_x$ pentablock terpolymers with various PNIPAm block length x onto the bare hydrophobic gold surface at 20 °C. It can be clearly seen that the adsorption kinetic and adsorption amount of $PNIPAm_x$-P123-$PNIPAm_x$ pentablock terpolymers were dependent on the length x of PNIPAm block. A densification adsorption process was observed for $PNIPAm_{10}$-P123-$PNIPAm_{10}$, as evident by the plot of $\Delta\Gamma_3/3$ *versus* $-\Delta f_3/3$ shown in Fig. 4B. The $\Delta\Gamma_3/3$ to $-\Delta f_3/3$ plot of $PNIPAm_{10}$-P123-$PNIPAm_{10}$ showed that the $\Delta\Gamma_3/3$ first increased with $-\Delta f_3/3$ and then decreased during the adsorption process (the arrows in Fig. 4B), indicating that the adsorbed $PNIPAm_{10}$-P123-$PNIPAm_{10}$ layer was densified with further adsorption. However, the thickness growth mode was observed for the adsorption behavior of $PNIPAm_{63}$-P123-$PNIPAm_{63}$ and $PNIPAm_{97}$-P123-$PNIPAm_{97}$, respectively, as evident by the linear relation of $\Delta\Gamma_3/3$ and $-\Delta f_3/3$. The adsorption kinetic of $PNIPAm_{63}$-P123-$PNIPAm_{63}$ or $PNIPAm_{97}$-P123-$PNIPAm_{97}$ with a thickness growth mode could be well described by using Langmuir model, given as[34]

$$\Delta f(t) \propto A(t) = A_\infty(1 - e^{-kt}) \quad (1)$$

where $A(t)$ is the surface coverage at time t, A_∞ is the equilibrium coverage, and k is the combination $k_a c_p + k_d$ with k_a being the intrinsic adsorption time constant, k_d being the intrinsic desorption time constant, and c_p being the concentration of polymer. Note that the frequency shift Δf is proportional to the surface coverage or adsorption amount. Eqn (1) fitted well the

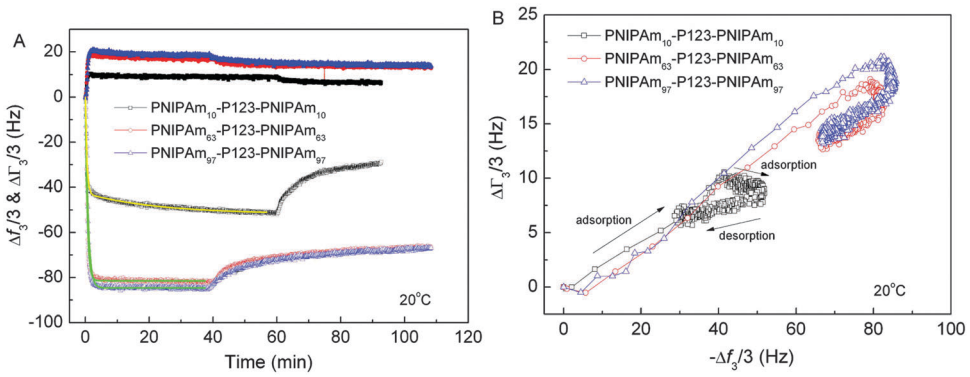

Fig. 4 (A) Frequency shifts ($\Delta f_3/3$, open symbols) and half-band-half width shifts ($\Delta\Gamma_3/3$, solid symbols) of the quartz crystals during the adsorption of $PNIPAm_x$-P123-$PNIPAm_x$ with various length x of PNIPAm block onto the bare hydrophobic gold surface at 20 °C. The green lines are fits with eqn (1). The yellow line is the fit with eqn (2). (B) The corresponding plots of half-band-half width shift $\Delta\Gamma_3/3$ *versus* negative frequency shift $-\Delta f_3/3$. The arrows are the guide to the eyes. The concentration of aqueous solution of the pentablock terpolymer was 0.5 mg mL^{-1}.

Table 2 Fitting parameters of eqn (1) and (2) for the adsorption kinetics of $PNIPAm_x$-P123-$PNIPAm_x$ onto the bare hydrophobic gold surfaces at 20 °C

Sample	A_1 (A_∞) (Hz)	k_1 (k) (min^{-1})	A_2 (Hz)	k_2 (min^{-1})	R^2
$PNIPAm_{10}$-P123-$PNIPAm_{10}$	−42.6 ± 0.1	2.27 ± 0.04	−9.19 ± 0.13	0.04	0.97
$PNIPAm_{63}$-P123-$PNIPAm_{63}$	−81.5 ± 0.1	1.69 ± 0.02	—	—	0.97
$PNIPAm_{97}$-P123-$PNIPAm_{97}$	−84.7 ± 0.1	1.21 ± 0.02	—	—	0.97

adsorption kinetic of $PNIPAm_{63}$-P123-$PNIPAm_{63}$ and $PNIPAm_{97}$-P123-$PNIPAm_{97}$ onto the bare hydrophobic gold surfaces at 20 °C (green lines in Fig. 4A). The two-step densification adsorption kinetic for adsorbed $PNIPAm_{10}$-P123-$PNIPAm_{10}$ layer could be described by a modified Langmuir model:

$$\Delta f(t) \propto A(t) = A_1(1 - e^{-k_1 t}) + A_2(1 - e^{-k_2 t}) \qquad (2)$$

where the physical meanings of k_1 and k_2 were similar with that of k and used to characterize the fast and slow adsorption processes, respectively. A_1 and A_2 presented the corresponding surface coverage contributed by the fast and slow adsorption processes, respectively. Eqn (2) fitted well the adsorption kinetic of $PNIPAm_{10}$-P123-$PNIPAm_{10}$ onto the bare hydrophobic gold surfaces at 20 °C (yellow line in Fig. 4A), which further supported the adsorption mechanism of densification adsorption process. The fitting parameters of eqn (1) and (2) were summarized in Table 2. It can be seen that the fast adsorption process mainly dominated the adsorption kinetics of $PNIPAm_{10}$-P123-$PNIPAm_{10}$. Furthermore, the adsorption time constant of the fast adsorption process decreased with increasing the length x of PNIPAm block. Previous report showed that the $PNIPAm_x$-P123-$PNIPAm_x$ pentablock terpolymers formed "associate" structures at temperatures below the LCST of PPO (like 20 °C), of which the size increased with increasing the length x of PNIPAm block.[30] The larger "associate" structures would result in a longer translational diffusion time constant, leading to the smaller adsorption rate of the polymer onto a surface.[13,14] As a result, the adsorption time constant of "associate" structures decreased with increasing the length x of PNIPAm block. The above results indicated that increasing the length x of PNIPAm block decreased the adsorption rate constant and shifted the adsorption mechanism from the densification adsorption process for $PNIPAm_{10}$-P123-$PNIPAm_{10}$ to the thickness growth mode for $PNIPAm_{63}$-P123-$PNIPAm_{63}$ and $PNIPAm_{97}$-P123-$PNIPAm_{97}$.

Effect of wetting property of gold surface

The surface properties of solid substrates will strongly affect the interactions between the polymer chains and substrates, which determine the adsorption behavior of the polymer onto the solid substrate. The above experiments were all carried out on a bare hydrophobic gold surface. In this subsection, the gold-electrode surfaces of the quartz crystals were further modified with thiols to give different surface chemistries and wetting properties. 1-Dodecanethiol ($HS(CH_2)_{11}CH_3$) and 11-mercapto-undecanol ($HS(CH_2)_{11}OH$) were used to achieve this purpose as described in the Experimental section. The contact angle measurements confirmed that the 1-dodecanethiol modified gold surface was hydrophobic with a contact angle of 108 ± 1° and the 11-mercaptoundecanol modified gold surface was hydrophilic with a contact angle of 25 ± 2°. Besides the wetting properties, the surface chemistries of the thiol-modified gold surfaces were also different. The surface chemical groups of dodecanethiol and mercaptoundecanol modified golds were $–CH_3$ groups and –OH groups, respectively.

Fig. 5 shows the adsorption behavior of $PNIPAm_{97}$-P123-$PNIPAm_{97}$ pentablock terpolymers onto the solid surface with various wetting and chemical properties at 20 °C. Note that the $PNIPAm_{97}$-P123-$PNIPAm_{97}$ pentablock terpolymer formed "associate" structures in aqueous solution at 20 °C. Fig. 5A indicates that the molecular chains of $PNIPAm_{97}$-P123-$PNIPAm_{97}$ pentablock terpolymers had strongest interactions with bare hydrophobic gold surface 20 °C, leading to the largest adsorption amounts, while the interactions between with $PNIPAm_{97}$-P123-$PNIPAm_{97}$ chains and $HS(CH_2)_{11}OH$ modified hydrophilic gold

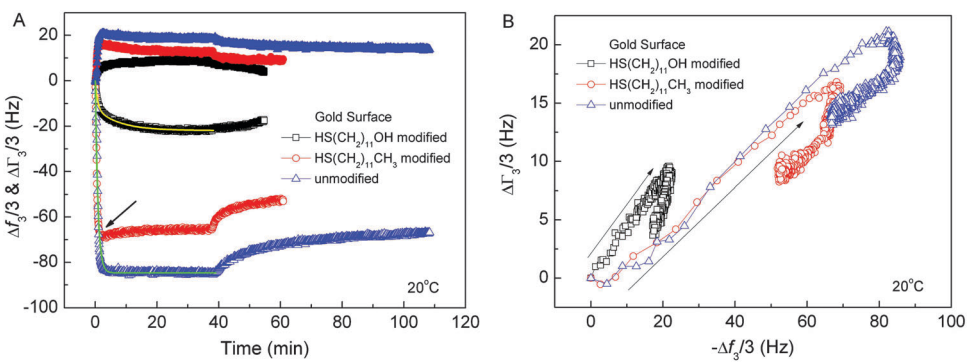

Fig. 5 (A) Frequency shifts ($\Delta f_3/3$, open symbols) and half-band-half width shifts ($\Delta\Gamma_3/3$, solid symbols) of the quartz crystals during the adsorption of $PNIPAm_{97}$-P123-$PNIPAm_{97}$ onto the gold surfaces with different wetting and chemical properties at 20 °C. The green line is the fit with eqn (1) for bare hydrophobic gold surface and the yellow line is the fit with eqn (2) for 11-mercaptoundecanol ($HS(CH_2)_{11}OH$) modified gold surface. (B) The corresponding plots of half-band-half width shift $\Delta\Gamma_3/3$ *versus* negative frequency shift $-\Delta f_3/3$. The arrows are the guide to the eyes. The concentration of $PNIPAm_{97}$-P123-$PNIPAm_{97}$ aqueous solution was 0.5 mg mL^{-1}.

surface were the weakest, leading to the smallest adsorption amounts. The adsorption mechanisms of $PNIPAm_{97}$-P123-$PNIPAm_{97}$ onto the hydrophobic gold surfaces (including unmodified and $HS(CH_2)_{11}CH_3$ modified) and hydrophilic gold surface ($HS(CH_2)_{11}OH$ modified) were the thickness growth mode and densification adsorption process, respectively, as indicated by the plots $\Delta\Gamma_3/3$ *vs.* $-\Delta f_3/3$ (Fig. 5B). As the results, eqn (1) could be used to well fit the frequency shift of the quartz crystals during the adsorption of $PNIPAm_{97}$-P123-$PNIPAm_{97}$ onto bare gold surface (green line in Fig. 5A). Instead, eqn (2) could well describe the adsorption of $PNIPAm_{97}$-P123-$PNIPAm_{97}$ onto $HS(CH_2)_{11}OH$ modified hydrophilic gold surface (yellow line in Fig. 5A). Interestingly, for $HS(CH_2)_{11}CH_3$ modified hydrophobic gold surface, there was a slight desorption phenomenon after the maximum adsorption during the adsorption process, as indicated by the arrow in Fig. 5A. Possibly, there were entangled interactions among the surface graft $HS(CH_2)_{11}CH_3$ chains and the adsorbed $PNIPAm_{97}$-P123-$PNIPAm_{97}$ chains. The rearrangement of conformation of $HS(CH_2)_{11}CH_3$ chains and adsorbed pentablock terpolymer chains might release the dis-entangled and weak adsorbed pentablock terpolymer chains, resulting in the observed desorption phenomenon before reaching the equilibrium state. Fig. 5B also indicates that the adsorbed pentablock terpolymer layer on a hydrophilic gold surface was softer than those on hydrophobic gold surfaces at 20 °C.

Interestingly, at the LCST of PNIPAm block, *i.e.* 34.7 °C, complex adsorption behavior of $PNIPAm_{97}$-P123-$PNIPAm_{97}$ was observed not only on hydrophobic gold surfaces but also on a hydrophilic gold surface, as shown in Fig. 6. The frequency shifts at adsorption equilibrium on different gold surfaces before rinsing were in order of $HS(CH_2)_{11}CH_3$ modified hydrophobic gold surface > bare (unmodified) hydrophobic gold surface > $HS(CH_2)_{11}OH$ modified hydrophilic gold surface. During rinsing step with de-ionized water, large desorption of $PNIPAm_{97}$-P123-$PNIPAm_{97}$ from the $HS(CH_2)_{11}CH_3$ modified hydrophobic gold surface was observed. After rinsing, the adsorption amounts on the unmodified and modified hydrophobic gold surfaces were similar. These results might suggest that the premicellar associative adsorption happened at the LCST of PNIPAm block regardless of the surface wetting properties of the substrates, leading to large adsorption amounts. It was understandable because the premicellar surface association was mainly determined by the chain conformation of $PNIPAm_{97}$-P123-$PNIPAm_{97}$ in aqueous solution.

Fig. 7 shows the adsorption behavior of $PNIPAm_{97}$-P123-$PNIPAm_{97}$ pentablock terpolymers onto the three gold substrates with various surface wetting and chemical properties at 45 °C. Note that the $PNIPAm_{97}$-P123-$PNIPAm_{97}$ pentablock terpolymers formed micelles with hydrophobic PNIPAm and PPO blocks as cores and soluble PEO blocks as coronas at temperature higher than the LCST of PNIPAm block.[30] As expected, the hydrophilic PEO corona chains had strong interactions with hydrophilic $HS(CH_2)_{11}OH$, leading to the largest adsorption amounts of $PNIPAm_{97}$-P123-$PNIPAm_{97}$ micelles on $HS(CH_2)_{11}OH$ modified hydrophilic gold surface. For $HS(CH_2)_{11}CH_3$ modified hydrophobic gold surface, the adsorption amount of $PNIPAm_{97}$-P123-$PNIPAm_{97}$ micelles was the smallest. Furthermore, the mechanism of the densification adsorption process was observed for the adsorption of $PNIPAm_{97}$-P123-$PNIPAm_{97}$ micelles onto the three gold surfaces studied here regardless of the surface wetting and chemical properties.

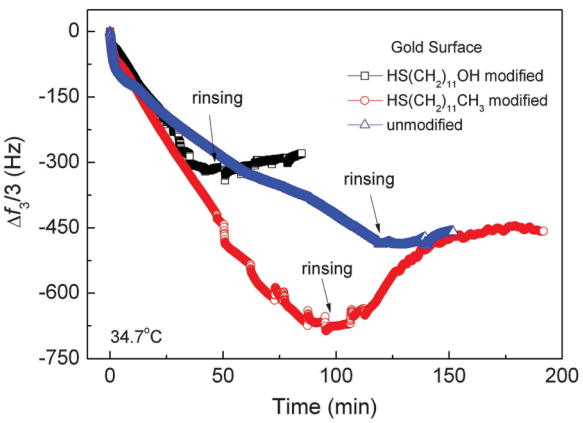

Fig. 6 Frequency shifts ($\Delta f_3/3$) of the quartz crystals during the adsorption of $PNIPAm_{97}$-P123-$PNIPAm_{97}$ onto the gold surfaces with different wetting properties at 34.7 °C. The concentration of $PNIPAm_{97}$-P123-$PNIPAm_{97}$ aqueous solution was 0.5 mg mL^{-1}.

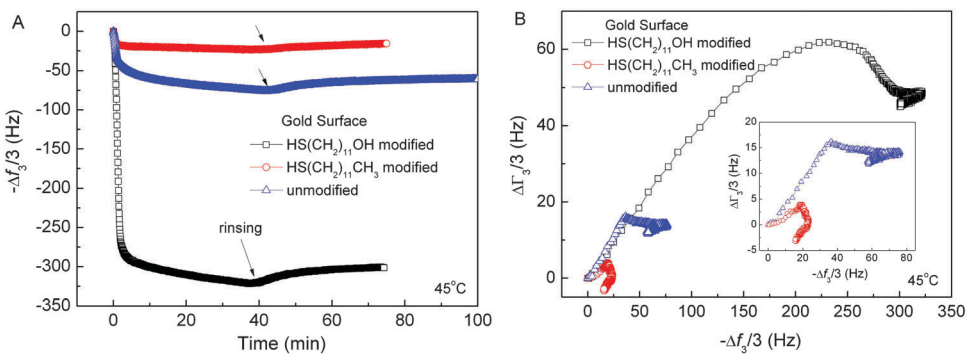

Fig. 7 (A) Frequency shifts $\Delta f_3/3$ of the quartz crystal during the adsorption of $PNIPAm_{97}$-P123-$PNIPAm_{97}$ onto the gold surfaces with different wetting properties at 45 °C. (B) The corresponding plots of half-band-half width shift $\Delta\Gamma_3/3$ *versus* negative frequency shift $-\Delta f_3/3$. The concentration of $PNIPAm_{97}$-P123-$PNIPAm_{97}$ aqueous solution was 0.5 mg mL^{-1}.

Clearly, the results of Fig. 5–7 indicated that the surface wetting and chemical properties of substrates exhibited a strong influence on the adsorption of $PNIPAm_{97}$-P123-$PNIPAm_{97}$ pentablock terpolymer. The adsorption amounts were dependent on the interactions of pentablock terpolymer chains and the substrates, which were dominated by the conformation of the pentablock terpolymer chains in aqueous solution.

Conclusions

The adsorption behavior of three pentablock terpolymer $PNIPAm_x$-P123-$PNIPAm_x$ with x of 10, 63 and 97 on the gold substrates was systematically investigated using a quartz crystal microbalance (QCM). The results indicated that the adsorption mechanisms were mainly dependent on the chain conformation of the pentablock terpolymers in dilute aqueous solutions at various temperatures and the surface wetting and chemical properties of the gold substrates. Increasing the solution concentration did not alter the adsorption mechanism of thickness growth mode but increase the adsorption amount of $PNIPAm_{97}$-P123-$PNIPAm_{97}$ on bare (unmodified) gold substrate. Increasing the length x of PNIPAm block decreased the adsorption rate constant and shifted the adsorption mechanism from the densification adsorption process for $PNIPAm_{10}$-P123-$PNIPAm_{10}$ to the thickness growth mode for $PNIPAm_{63}$-P123-$PNIPAm_{63}$ and $PNIPAm_{97}$-P123-$PNIPAm_{97}$ on bare (unmodified) gold substrate. The adsorption mechanisms of $PNIPAm_{97}$-P123-$PNIPAm_{97}$ at 20 °C on the hydrophobic and hydrophilic gold surfaces were the thickness growth mode and densification adsorption process, respectively. The adsorption amounts of $PNIPAm_{97}$-P123-$PNIPAm_{97}$ at 20 °C were in the order of $HS(CH_2)_{11}CH_3$ modified hydrophobic gold surface > bare (unmodified) hydrophobic gold surface > $HS(CH_2)_{11}OH$ modified hydrophilic gold surface. Complex adsorption behavior with large adsorption amounts was observed at the LCST of PNIPAm block, *i.e.* 34.7 °C, for adsorption of $PNIPAm_{97}$-P123-$PNIPAm_{97}$ not only on hydrophobic gold substrates but also on hydrophilic gold substrates. For adsorption of $PNIPAm_{97}$-P123-$PNIPAm_{97}$ at 45 °C, the adsorption mechanism was a densification adsorption process regardless of the surface wetting and chemical properties of the gold substrate.

Acknowledgements

The authors thank the National Natural Science Foundation of China (No. 20874087 and 21074114) for financial support. B. Du thanks the Alexander-von-Humboldt foundation for donation of the Quartz Crystal Microbalance.

References

1 K. Sakai, M. Vamvakaki, E. G. Smith, E. J. Wanless, S. P. Armes and S. Biggs, *J. Colloid Interface Sci.*, 2008, **317**, 383–394.
2 Y. Yan, X. Zhou, J. Ji, L. Yan and G. Zhang, *J. Phys. Chem. B*, 2006, **110**, 21055–21059.
3 K. Sakai, E. G. Smith, G. B. Webber, M. Baker, E. J. Wanless, V. Bütün, S. P. Armes and S. Biggs, *Langmuir*, 2006, **22**, 8435–8442.
4 E. J. Park, D. D. Draper and N. T. Flynn, *Langmuir*, 2007, **23**, 7083–7089.
5 I. G. Sedeva, D. Fornasiero, J. Ralston and D. A. Beattie, *Langmuir*, 2009, **25**, 4514–4521.
6 A. Naderi, J. Iruthayaraj, T. r. Pettersson, R. a. Makuška and P. M. Claesson, *Langmuir*, 2008, **24**, 6676–6682.
7 G. Liu and G. Zhang, *J. Phys. Chem. B*, 2004, **109**, 743–747.
8 G. Liu, H. Cheng, L. Yan and G. Zhang, *J. Phys. Chem. B*, 2005, **109**, 22603–22607.
9 M. A. Plunkett, Z. Wang, M. W. Rutland and D. Johannsmann, *Langmuir*, 2003, **19**, 6837–6844.
10 G. Zhang, *Macromolecules*, 2004, **37**, 6553–6557.
11 Y. Kikkawa, K. Yamashita, T. Hiraishi, M. Kanesato and Y. Doi, *Biomacromolecules*, 2005, **6**, 2084–2090.
12 B. Wu, K. Wu, P. Wang and D.-M. Zhu, *J. Phys. Chem. C*, 2006, **111**, 1131–1135.
13 D.-M. Zhu, K. Wu, B. Wu, P. Wang, J. Fang, Y. Hou and G. Zhang, *J. Phys. Chem. C*, 2007, **111**, 18679–18686.
14 K. Wu, B. Wu, P. Wang, Y. Hou, G. Zhang and D.-M. Zhu, *J. Phys. Chem. B*, 2007, **111**, 8723–8727.
15 M. R. Nejadnik, A. L. J. Olsson, P. K. Sharma, H. C. van der Mei, W. Norde and H. J. Busscher, *Langmuir*, 2009, **25**, 6245–6249.
16 X. G. Briones, M. V. Encinas, D. F. S. Petri, J. E. Pavez, R. A. Tapia, M. Yazdani-Pedram and M. D. Urzúa, *Langmuir*, 2011, **27**, 13524–13532.
17 M. Malmsten, P. Linse and T. Cosgrove, *Macromolecules*, 1992, **25**, 2474–2481.
18 K. Eskilsson and F. Tiberg, *Macromolecules*, 1998, **31**, 5075–5083.
19 P. Brandani and P. Stroeve, *Macromolecules*, 2003, **36**, 9492–9501.
20 P. Brandani and P. Stroeve, *Macromolecules*, 2003, **36**, 9502–9509.
21 S. Bhattacharya, H. P. Hsu, A. Milchev, V. G. Rostiashvili and T. A. Vilgis, *Macromolecules*, 2008, **41**, 2920–2930.
22 H. Chen, C. Peng, Z. Ye, H. Liu, Y. Hu and J. Jiang, *Langmuir*, 2007, **23**, 2430–2436.
23 X. Liu, A.-H. Vesterinen, J. Genzer, J. V. Seppälä and O. J. Rojas, *Langmuir*, 2011, **27**, 9769–9780.
24 Y. Lu, X. Zhang, Z. Fan and B. Du, *Polymer*, 2012, **53**, 3791–3801.
25 A. Corsi, A. Milchev, V. G. Rostiashvili and T. A. Vilgis, *J. Chem. Phys.*, 2005, **122**, 094907.
26 Y. A. Kriksin, P. G. Khalatur and A. R. Khokhlov, *J. Chem. Phys.*, 2005, **122**, 114703.
27 K. Sumithra, M. Brandau and E. Straube, *J. Chem. Phys.*, 2009, **130**, 234901.
28 A. Corsi, A. Milchev, V. G. Rostiashvili and T. A. Vilgis, *J. Polym. Sci., Part B: Polym. Phys.*, 2006, **44**, 2572–2588.

29 A. Mei, X. Guo, Y. Ding, X. Zhang, J. Xu, Z. Fan and B. Du, *Macromolecules*, 2010, **43**, 7312–7320.
30 Y. Lu, T. Chen, A. Mei, T. Chen, Y. Ding, X. Zhang, J. Xu, Z. Fan and B. Du, *Phys. Chem. Chem. Phys.*, 2013, **15**, 8276–8286.
31 D. Johannsmann, *Phys. Chem. Chem. Phys.*, 2008, **10**, 4516–4534.
32 M. Lindheimer, E. Keh, S. Zaini and S. Partyka, *J. Colloid Interface Sci.*, 1990, **138**, 83–91.
33 P. Levitz and H. Van Damme, *J. Phys. Chem.*, 1986, **90**, 1302–1310.
34 D. S. Karpovich and G. J. Blanchard, *Langmuir*, 1994, **10**, 3315–3322.

